Cholesteric-nematic transition in an asymmetric strong-weak anchoring cell

Cholesteric-nematic transition in an asymmetric strong-weak anchoring cell

G. Barbero[1,*] and A. M. Scarfone[2,†]

[1]*Turin Polytechnical University in Tashkent, 17, Niyazov Str. Sobir Rakhimov district Tashkent, 100095 Uzbekistan*

[2]*ISC-CNR, Istituto dei Sistemi Complessi, Consiglio Nazionale delle Ricerche c/o Department of Applied Science and Technology, Politecnico di Torino, Corso Duca degli Abruzzi 24, 10129 Torino, Italy*

(Received 8 April 2013; revised manuscript received 4 June 2013; published 23 September 2013)

We discuss the cholesteric-nematic transition induced by an external field in a cell in the shape of a slab of finite thickness whose anchoring energy is infinitely strong on one surface and negligible on the other. The case where the surface orientations of the cholesteric director are parallel in the ground state is considered. In a sample of thickness ℓ, multiple of the natural periodicity of the system Λ, the number of complete twists in the cholesteric liquid crystal is reduced by increasing the strength of the external distorting field. The sequence of the field values for expelling complete twists accumulate as the strength of the field approaches a critical value. Beyond this critical value the system assumes an unwinding configuration going toward a uniform structure, corresponding to nematic phase. Generalization of the results to the weak-weak anchoring cell case is also discussed. In our analysis the anisotropic part of the surface energy is assumed or very large or very small with respect to the total energy per unit surface due to the bulk distortion induced by the magnetic field.

DOI: 10.1103/PhysRevE.88.032505 PACS number(s): 61.30.Dk, 64.70.M−

I. INTRODUCTION

Liquid crystals form a distinct phase of matter that may exist in several configurations and whose structure is intermediate between those of liquid and crystal. They possess some typical properties of a liquid, like fluidity, inability to support shear, formation, and coalescence of droplets as well as anisotropy in optical, electrical, and magnetic properties, and periodic arrangement of molecules in one spatial direction, among many, that are typical of crystalline state [1]. Liquid crystals may exhibit several phases like the nematic phase, the smectic phase, the cholesteric phase, the blue phase, the columnar or discotic phase, and others.

In the nematic phase the molecules have no positional order but tend to align parallel to a common direction, called the nematic director. Conversely, in the cholesteric phase, the alignment of the molecules varies in direction throughout the medium in a regular way. The configuration is precisely what one would obtain by twisting about the x axis a nematic liquid crystal initially aligned along the y axis.

Due to this difference in the internal structure, nematic liquid crystals (NLCs) and cholesteric liquid crystals (CLCs) show different physical proprieties which make them of a certain interest for their potential technological applications. In particular, the helical structure of CLCs confers unique electro-optic and photonic properties attractive for applications in switchable diffraction gratings, eyeglasses with voltage-controlled transparency, temperature visualization, mirrorless lasing, and beam steering and beam shaping devices, as well as in the construction of reflective displays. The design of these devices requires the study of electrical and optical properties of liquid crystals in great detail.

Due to the dielectric or diamagnetic anisotropy of the single molecules forming the liquid crystal, the helix structure of CLC may be modified by the application of an external field. In particular, a sufficiently intense electric or magnetic field can induce the transition of a CLC to the nematic phase. Therefore, understanding these structures and the transitions between them is of practical interest and of fundamental importance as demonstrated by the current literature [2–15].

The problem of untwisting a CLC about its helical axis was studied theoretically by de Gennes long ago [16]. He considered the case of an unbounded sample. By evaluating the minima of the energy over one twist, he has shown that at a well-defined critical field strength the pitch of the helical distortion diverges. This leads to the conclusion that over the critical field the CLC has an untwisted structure such that the director becomes almost constant in space like in the nematic phase [17–20]. A similar calculation, by assuming a sample of finite thickness in the strong anchoring hypothesis was discussed in Refs. [21–26], to cite a few, while the action of a surface field combined with an external bulk field at transitions has been investigated in Ref. [27].

In Refs. [28,29], we have generalized previous studies, relevant to the CLC → NLC transition induced by a magnetic field, by assuming strong anchoring on the limiting surfaces of the cell. In this framework, it has been shown that, as the external field increases in its strength, the system expels one twist at a time until a certain critical value is reached, beyond which the system passes from the cholesteric to the nematic phase. No similar theoretical analysis for a sample limited by weak anchoring has been reported until now.

In the present work we consider a the CLC → NLC transition induced by a magnetic field in a cell characterized by strong anchoring on one surface and negligible anchoring on the other. The case where the anchoring energy is negligible on both surfaces is also discussed. This analysis is a natural extension of the cases discussed in Refs. [28,29]. Since we limit our analysis to the case in which on one of the surface the anchoring is negligible and on the other strong or also negligible we do not need to assume a particular form for the anisotropic part of the surface energy. In the following we will consider, for clarity, the case where the surface energy

*Department of Applied Science and Technology, Politecnico di Torino, Corso Duca degli Abruzzi 24, 10129 Torino, Italy.

†Corresponding author: antoniomaria.scarfone@cnr.it

is proportional to the sinus square of the angular deviation of the surface twist angle from the easy axis. In this framework we obtain general formulas describing the deformation of the CLC in the presence of an external distorting magnetic field. However, a detailed analysis is presented only for the situation where the anchoring energy strength tends to zero. Consequently, the presented analysis is valid for all cases where the anchoring energy is negligible with respect to the elastic energy related to the distortion and with respect to the anisotropic part of the magnetic energy describing the coupling between the external magnetic field and the CLC. An analysis on the influence of the surface energy on the CLC $\rightarrow$ N transition induced by a magnetic field can be done using the formalism presented in the paper, and it is obviously dependent on the functional form of its anisotropic part and, hence, of reduced generality. For this reason we limited our investigation to the extreme cases of negligible-negligible and negligible-strong anchoring energy conditions.

The plane of the paper is the following. In the next Sec. II, we introduce the formalism used to deal with the problem of the CLC $\rightarrow$ NLC transition. In Sec. III, we analyze in details the effect of the boundary conditions on the system. The question of the stable equilibrium configuration for a given value of the external field is discussed in Sec. IV. Section V contains the main results of our work. We study, by numerical methods, the equilibrium configuration of the system for a given value of the distorting field. There, we show that, as the strength of the field increases, the system expels twists one by one up to a critical field, beyond which the system assumes a untwisted configuration. Finally, in Sec. VI, we generalize briefly our discussion to the cases of a weak-weak anchoring cell system. Conclusions are reported in Sec. VII.

II. POSITION OF THE PROBLEM

The experimental arrangement used to study the CLC $\rightarrow$ NLC transition is made by a CLC confined between two flat glass substrates treated in such a way to align the molecules at the interface along a well-defined direction called the easy direction. An electric or magnetic field is then used to switch the liquid crystal between different textures. In this situation, when the external field is off, the CLC has a twisted helicoidal director field in the ground state that is characterized by the axis of molecular twist, named the helical axis, and by the spatial period over which the liquid crystal molecules twist, named the cholesteric pitch p [30].

In the following we assume the system, infinite in the x, y directions, confined in the z direction by two parallel plates located at $z = 0$ and $z = \ell$. The helical axis is perpendicular to the xy plane. The nematic director, $\boldsymbol{n}$, is aligned parallel to the y axis on the limiting surfaces, $\boldsymbol{n}(0) = \boldsymbol{n}(\ell) = \boldsymbol{j}$, where $\boldsymbol{i}$ and $\boldsymbol{j}$ are the unit vectors along the x and y axes, respectively. The thickness of the sample is $\ell = \Lambda N$, where $\Lambda = p/2$ is the natural cholesteric half-pitch and N is the complete half-pitch number. In this way, the intrinsic twist deformation of CLC is described by the twist angle $\phi(z)$ formed by $\boldsymbol{n}$ with the y axis. In the absence of distorting field, the system has an integer number N of π twists, with $\phi_N(z) = (\pi/\Lambda)\, z$. The external field is assumed in the $\boldsymbol{j}$ direction so $\boldsymbol{H} = H\, \boldsymbol{j}$.

Hereinafter, we rescale the z coordinate according to $\zeta = z/\ell$ in such a manner that $0 \leqslant \zeta \leqslant 1$. We denote by $\lambda = \Lambda/\ell = 1/N$ the density of the π twist in the sample, representing the number of π twists per unit length in the absence of external field.

Within this formalism, the bulk energy density is [16]

$$f[\varphi] = \frac{K}{2\,\ell}\left[\left(\frac{d\varphi}{d\zeta} - \frac{\pi}{\lambda}\right)^2 - \frac{1}{\xi^2}\cos^2\varphi\right], \tag{2.1}$$

where $\varphi(\zeta) \equiv \phi(z)$, K is the elastic constant for twist deformation, and $\xi = (K/\chi_a)^{1/2}/H\,\ell$ is the dimensionless magnetic coherence length. In the definition of ξ we indicate by $\chi_a = \chi_\parallel - \chi_\perp$, where $\parallel$ and $\perp$ refer to $\boldsymbol{n}$, the macroscopic diamagnetic anisotropy of the CLC.

The first contribution to $f[\varphi]$ is of elastic origin, and it is related to the spontaneous twist related to the molecular structure of the CLC, whereas the second contribution takes into account the magnetic energy related to the anisotropic coupling of the magnetic field with the CLC.

The anisotropic part of the surface energy density on the surface characterized by the weak anchoring is approximated by the functional form [31]

$$g(\varphi) = -\frac{w}{2}\cos^2\varphi, \tag{2.2}$$

where w is the anchoring energy strength. As discussed above in the following we will be interested in the case where $w \to 0$, that corresponds to the situation in which the surface energy is negligible with respect to the bulk energy, per unit surface, related to the elastic and magnetic properties of the CLC in the presence of an external magnetic field. In this limit, obviously, the form $g(\varphi)$ is inessential.

For a given profile $\varphi(\zeta)$ the total energy per unit surface $G[\varphi]$ is given by

$$G[\varphi] = \int_0^1 f[\varphi]\, d\zeta + g(\varphi(1)), \tag{2.3}$$

where we assumed strong anchoring at the limiting surface in $\zeta = 0$. Also in this case, the assumption of strong surface energy does not imply any well-defined form for the functional form for the anisotropic part of the surface energy density. If, by means of an external action, we modify the profile of the twist angle from $\varphi(\zeta)$ to $\hat{\varphi}(\zeta) = \varphi(\zeta) + \delta\varphi(\zeta)$ the variation of the total energy per unit surface is

$$\delta G[\varphi] = \int_0^d \left[\frac{\partial f}{\partial \varphi} - \frac{d}{d\zeta}\left(\frac{\partial f}{\partial \varphi'}\right)\right]\delta\varphi\, d\zeta + \left(\frac{\partial f}{\partial \varphi'} + \frac{dg}{d\phi}\right)\Bigg|_1 \delta\phi(1), \tag{2.4}$$

where $\varphi' = d\varphi/d\zeta$. From the physical point of view, the first term in the right-hand side represents the work done by the bulk torque during the deformation from $\varphi(\zeta)$ to $\varphi(\zeta) + \delta\varphi(\zeta)$, whereas the second contribution is the work due to the surface torque to induce the surface deformation. From the form of the second term it is clear that the effective surface torque has an elastic contribution, which represents the torque transmitted to the surface from the bulk, and a torque due to the presence of the surface easy axis, related to the anisotropic part of the surface energy. If the profile $\varphi(\zeta)$ represents a profile of

equilibrium, the bulk density of torque, as well the surface density of torque, are identically zero. In this case $\delta G[\varphi] = 0$ for all $\delta\varphi$, and from Eq. (2.4) we get

$$\frac{\partial f}{\partial \varphi} - \frac{d}{d\zeta}\left(\frac{\partial f}{\partial \varphi'}\right) = 0 \tag{2.5}$$

for the bulk and

$$\left.\frac{\partial f}{\partial \varphi'}\right|_1 + \left.\frac{dg}{d\varphi}\right|_1 = 0 \tag{2.6}$$

for the boundary condition. The analysis presented above is based on the principle of the virtual work, according to which the variation of total energy for a small modification of the profile around a state of equilibrium vanishes identically. From the mathematical point of view, using the language of the variational calculus, the first variation of the functional representing the total energy per unit surface has to be identically zero for all $\delta\varphi(\zeta)$ continuous with its first derivative.

Explicitly, the bulk equation becomes

$$\frac{d^2\varphi}{d\zeta^2} - \frac{1}{\xi^2}\sin\varphi\cos\varphi = 0, \tag{2.7}$$

stating that in the stable state the bulk density of torque is identically zero. This means that in the stable state the restoring torque, of elastic origin, balances the distorting torque of magnetic origin. Furthermore, for the boundary conditions we get

$$\left.\frac{d\varphi}{d\zeta}\right|_1 - \frac{\pi}{\lambda} = -\frac{1}{2L}\sin(2\varphi(1)), \tag{2.8}$$

where $L = K/w\,\ell$ is the dimensionless extrapolation length [32], together with

$$\varphi(\zeta)|_0 = 0, \tag{2.9}$$

on the surface characterized by strong anchoring. Equation (2.8) indicates that in the state of equilibrium the torque transmitted by the bulk to the surface is equilibrated by the surface torque due to the easy direction. In a similar manner, Eq. (2.9) indicates that the surface torque is so strong to maintain the surface director aligned along the easy axis.

In the following, we assume that the surface energy at $\zeta = 1$ is negligible with respect to the bulk energy due to the deformation produced by the external field. In this case, we pose in Eq. (2.8) $w = 0$, and hence $L \to \infty$, so this equation reduces to

$$\left.\frac{d\varphi}{d\zeta}\right|_1 = \frac{\pi}{\lambda}. \tag{2.10}$$

Therefore, the surface director at $\zeta = 1$ is unconstrained and the orientation of the system on the limiting surface is the one transmitted by the bulk to the surface. However, since the system is limited, its translation symmetry is broken, a fact that is reflected by Eq. (2.10), which fixes the slope of the twist angle on the weakly anchored surface.

III. GENERAL CONSIDERATIONS ON THE BOUNDARY CONDITIONS

As discussed in Ref. [28], Eq. (2.7) admits the first integral

$$\left(\frac{d\varphi}{d\zeta}\right)^2 - \frac{1}{\xi^2}\sin^2\varphi = \frac{\kappa}{\xi^2}, \tag{3.1}$$

where $\kappa \equiv \kappa(\xi)$ is an integration constant to be determined.

From Eq. (3.1), by assuming positive helicity, we get

$$\frac{d\varphi}{d\zeta} = \frac{1}{\xi}\sqrt{\kappa + \sin^2\varphi}, \tag{3.2}$$

and accounting for the boundary conditions (2.10), in the limit of vanishing external field $\xi \to \infty$, we have

$$\lim_{\xi\to\infty}\frac{\kappa}{\xi^2} = \left(\frac{\pi}{\lambda}\right)^2, \tag{3.3}$$

indicating that, in the considered limit, $\kappa \propto \xi^2$.

On the other hand, by solving Eq. (3.2) with respect to κ and recalling again Eq. (2.10) we obtain

$$\kappa = \left(\frac{\pi}{\lambda}\xi\right)^2 - \sin^2\varphi(1). \tag{3.4}$$

Clearly, when the distorting field goes to zero,

$$\Delta\varphi \to N\,\pi, \tag{3.5}$$

where

$$\Delta\varphi = \varphi(1) - \varphi(0) \equiv \varphi(1), \tag{3.6}$$

is the total twist angle. In the same limit of negligible external field we derive the shape of the twist angle

$$\varphi(\zeta) = \frac{\pi}{\lambda}\zeta, \tag{3.7}$$

as it follows by solving Eq. (2.7) for $\xi \to \infty$. This is, of course, in agreement with Eq. (3.5), by recalling that $\lambda = 1/N$.

On the contrary, for finite ξ, i.e., $H \neq 0$, the twist angle profile $\varphi(\zeta)$ is distorted and its value on the limiting surface at $\zeta = 1$ changes depending on the strength of the field ξ. In this case, we rewrite Eq. (3.5) as

$$\Delta\varphi = N\,\pi - \delta, \tag{3.8}$$

where δ must be determined by the bulk equation (3.2) together with the boundary conditions (2.9) and (2.10).

We rewrite Eq. (3.4) as

$$\kappa = \left(\frac{\pi}{\lambda}\xi\right)^2 - \sin^2\delta, \tag{3.9}$$

since, in this case, $\varphi(1) \equiv \Delta\varphi$ and from Eq. (3.2) we obtain the following differential equation:

$$\frac{d\varphi}{d\zeta} = \frac{1}{\xi}\sqrt{\left(\frac{\pi}{\lambda}\xi\right)^2 - \sin^2\delta + \sin^2\varphi}, \tag{3.10}$$

from which we get

$$\int_0^{N\pi-\delta}\frac{d\varphi}{\sqrt{\left(\frac{\pi}{\lambda}\xi\right)^2 - \sin^2\delta + \sin^2\varphi}} = \frac{1}{\xi}. \tag{3.11}$$

The integral in the left-hand side can be easily evaluated in terms of incomplete elliptic functions $\mathcal{F}(x,k)$ [33] by posing

$$f(\xi,m)=\frac{1}{\sqrt{\kappa}}\,\mathcal{F}\left(m,-\frac{1}{\kappa}\right), \tag{3.12}$$

where

$$\mathcal{F}(x,k)=\int_0^x \frac{d\alpha}{\sqrt{1-k^2\,\sin^2\alpha}}. \tag{3.13}$$

In this way, the possible values of δ are solutions of the transcendent equation

$$f(\xi,N\,\pi-\delta)=\frac{1}{\xi}. \tag{3.14}$$

In the limit of small H, i.e., large ξ, we can expand the integrand in Eq. (3.11) up to the first order in ξ^{-2} to obtain

$$1=\frac{\lambda}{\pi}\,(N\,\pi-\delta)-\frac{1}{4\,\xi^2}\left(\frac{\lambda}{\pi}\right)^3 \times\left[\cos(2\,\delta)\,(N\,\pi-\delta)+\sin(2\,\delta)\right], \tag{3.15}$$

and, recalling that $\lambda=1/N$, at the lowest order we have

$$\delta=-\frac{N\,\pi}{1+(2\,N\pi\,\xi)^2}. \tag{3.16}$$

As expected, $\delta\to 0$ in the $\xi\to\infty$ limit, although it takes negative value. Therefore, at the onset of the distorting external field the total twist angle increases.

Conversely, as the distorting field grows, i.e., for $\xi\to 0$, the constant κ becomes negative, as it follows from Eq. (3.9). Consequently, function $f(\xi,N\,\pi-\delta)$ takes imaginary values for certain δ and Eq. (3.14), in these cases, does not have real solutions. By inspection, $f(\xi,N\,\pi-\delta)$ is a modulated function, as depicted in Fig. 1, whose local maxima increase, in absolute value, as the value of ξ grows. Consequently, the number of possible solutions of δ, given by the intersection of $f(\xi,N\,\pi-\delta)$ with the horizontal line, at $1/\xi$, increases too. Vertical asymptotes appear in correspondence of negative values of κ. They occur at

$$\delta=\pm\arcsin\left(\frac{\pi}{\lambda}\,\xi\right). \tag{3.17}$$

In particular, for $\xi\to 0$ the solutions of Eq. (3.14) are localized in

$$\delta=m\pi, \tag{3.18}$$

where m is an integer. It labels the branches of all possible solutions of Eq. (3.14).

As can be see from Fig. 1(c), the number of solutions for $m>0$ is limited by the condition $m\leqslant N$, whereas there are an infinite number of solutions for $m<0$. However, solutions corresponding to negative branches represent system configurations with a total twist number greater than N, since, in these cases, $\Delta\varphi=N\,\pi-\delta>N\,\pi$. These configurations turn out to be energetically unstable, as will be discussed in Sec. V. In the following, we discard negative branches and limit our considerations only to $0\leqslant m\leqslant N$. In this way, m represents the number of expelled twists by the system.

In Fig. 2, are depicted the solutions of Eq. (3.14) for a system of $N=4$ twists vs the distorting field ξ. For large values of ξ the unique solution of δ takes negative values, as mentioned above. This means that, initially, the unique possible stable configuration is related to the main branch $m=0$ with an increasing total twist numbers. However, new branches become available whenever the strength of the field reduced below a threshold ξ_m whose value depends on the order of the branch m.

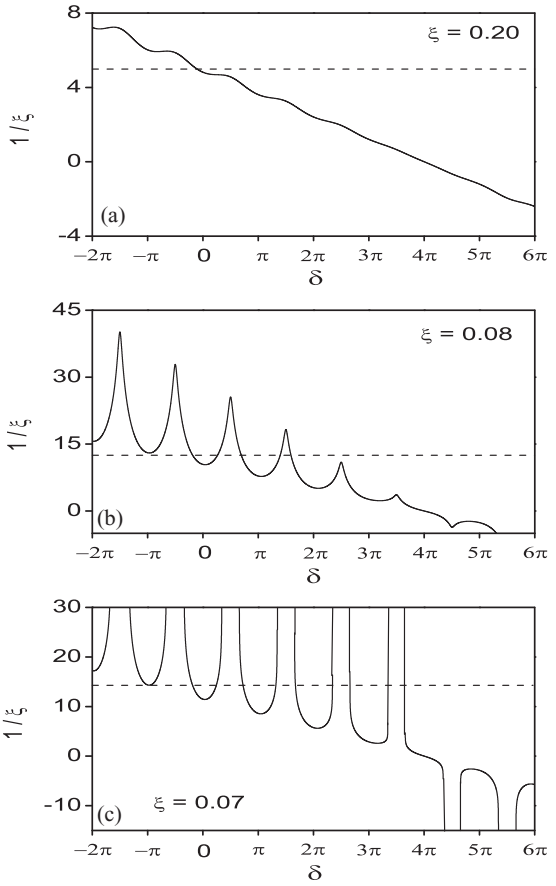

FIG. 1. Plot of the $f(\xi,N\,\pi-\delta)$ vs δ for several values of the external field ξ in a system with $N=4$ twists. The horizontal dashed line correspond to the value of $1/\xi$. Solutions of Eq. (3.14) are in correspondence of the intersections between the dashed lines and the solid line.

In this way, the number of twists may reduce when high-order branches become available in the system. We also observe that the onset of high-order branches becomes closer and closer as $\xi\to 0$. This is shown in Fig. 2 for the case of $N=4$. The threshold values ξ_m, with $m=1,2,3$ and 4, approach to a critical point $\xi_c\equiv\xi_N$. In particular, for a realistic CLC, with $N\approx 100$, the expulsion of twists occur in avalanche as the external field approaches the critical value ξ_c.

IV. STABLE STATES

The next step is to evaluate the total energy of the system for each possible configuration of a given value ξ. Stable equilibrium configuration corresponds to the minimum minimorum of the energy, evaluated over all possible solutions of Eq. (3.14).

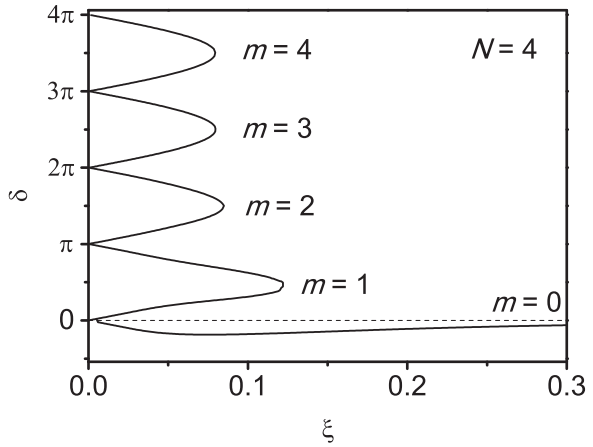

FIG. 2. Shape of δ vs ξ for a system with $N = 4$ twists. Solutions corresponding to $m < 0$ are not plotted. The dashed line represents the asymptotic behavior of the main solution ($m = 0$) for $\xi \to \infty$.

To do this, we introduce the reduced total energy per unit surface $\mathcal{G} = (2\,\ell/k)\,G$, given by

$$\mathcal{G}[\varphi] = \int_0^1 \left[\left(\frac{d\varphi}{d\zeta} - \frac{\pi}{\lambda}\right)^2 - \frac{1}{\xi^2}\cos^2\varphi\right] d\zeta, \qquad (4.1)$$

obtained from Eqs. (2.1) and (2.3). Passing to the twist angle variable we rewrite this equation in

$$\mathcal{G}[\varphi] = \int_0^{N\pi-\delta} \left[\left(\frac{d\varphi}{d\zeta} - \frac{\pi}{\lambda}\right)^2 - \frac{1}{\xi^2}\cos^2\varphi\right] \frac{d\varphi}{\varphi'}, \qquad (4.2)$$

where $\delta = \delta(\xi)$ is a solution of the boundary condition (3.14). As stated before, the actual twist profile is that corresponding to the minimum minimorum of $\mathcal{G}[\varphi]$ for all possible profile $\delta(\xi)$.

Evaluating the integral appearing in Eq. (4.2) we can write the reduced total energy as

$$\mathcal{G}[\varphi] = -\frac{1}{\xi^2}(1+\kappa) + \frac{\pi}{\lambda}\left[\frac{\pi}{\lambda} - 2\,(N\,\pi - \delta)\right] + 2\,\frac{\sqrt{\kappa}}{\xi}\,\mathcal{E}\left(N\,\pi - \delta, -\frac{1}{\kappa}\right), \qquad (4.3)$$

where

$$\mathcal{E}(x,k) = \int_0^x \sqrt{1 - k^2\,\sin^2\alpha}\,d\alpha, \qquad (4.4)$$

is the incomplete elliptic integral of the second kind [33].

Before considering the stable states related to $\mathcal{G}[\varphi]$, let us analyze the asymptotical configuration occurring in the $\xi \to 0$ limit (strong external field). In this situation, in the bulk the director is practically oriented along the field, with φ very close to 0 or to π. This corresponds to an almost nematic configuration and an approximate solution of Eq. (2.7) can be obtained from its linearization,

$$\frac{d^2\varphi}{d\zeta^2} - \frac{\varphi}{\xi^2} = 0, \qquad (4.5)$$

whose solution, satisfying the boundary conditions (2.9) and (2.10), is

$$\varphi(\zeta) = \varphi_0\,\sinh\left(\frac{\zeta}{\xi}\right), \qquad (4.6)$$

with

$$\varphi_0 = \frac{\pi}{\lambda}\,\frac{\xi}{\cosh(1/\xi)}. \qquad (4.7)$$

It is easy to show that solution (4.6) is energetically stable with respect to the uniform configuration $\varphi(\zeta) \equiv \varphi_u(\zeta) = 0$, $\forall\zeta \in [0, 1]$, which is achieved in the $\xi \to 0$ limit.

In fact, the reduced total energy for the uniform state φ_u is simply

$$\mathcal{G}[\varphi_u] = \left(\frac{\pi}{\lambda}\right)^2 - \frac{1}{\xi^2}. \qquad (4.8)$$

On the other hand, the total reduced energy related to the solution (4.6), in the limit of small ξ, can be written as

$$\mathcal{G}_0 = \mathcal{G}[\varphi_u] + \delta\mathcal{G}_0, \qquad (4.9)$$

where the energy due to the nonhomogeneity is

$$\delta\mathcal{G}_0 = -\frac{1}{2}\left(\frac{\pi}{\lambda}\right)^2 \frac{\sinh(2/\xi)}{\cosh^2(1/\xi)}, \qquad (4.10)$$

which is a negative definite quantity for $\xi > 0$.

Since the homogeneous state is stable with respect to the distorted one only if $\mathcal{G}_0 > \mathcal{G}[\varphi_u]$, it follows that uniform state is never an equilibrium stable configuration for any values of $\xi > 0$.

V. NUMERICAL ANALYSIS

Endowed with the numerical solutions of Eq. (3.14), we evaluate and compare the reduced total energy per unit surface for any possible curve $\delta(\xi)$. This is shown in Fig. 3 for a system containing $N = 4$ twists. We note that energy curves are monotonic and increase as $\xi \to \infty$. They are definite in the region $R_m \in (0, \xi_m)$, for $0 \leqslant m \leqslant N$.

The continuous line corresponds to the main branch $m = 0$ and represents the stable configuration for large values of ξ. However, as the strength of the external field increases, new energy levels become available in correspondence with the high-order branches. It is observed that, at the onset of any energy levels of highest-order, they have higher value than

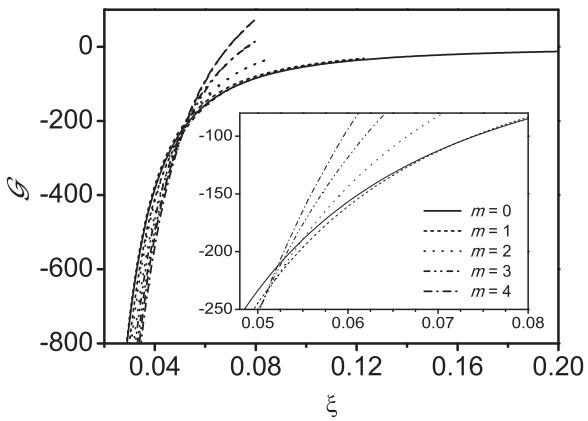

FIG. 3. Reduced total energy per unit surface vs the distorting field ξ for a $N = 4$ twists system. The insert reproduces, enlarged, the region including the intersection of the different branches. Energy curves corresponding to the negative branches are not plotted.

that corresponding to the energy levels of lowest-order branch. Actually, they decrease rapidly for $\xi \to 0$ so any high-order energy curve intersects the near next lower-order energy curve in a point $\xi_m^* < \xi_m$. Consequently, it is expected that the system transits in correspondence with ξ_m^* from the $(m-1)$ branch to the m branch. This corresponds actually to a reduction of the total twist number according to $N-(m-1) \to N-m$.

The final transition occurs when the critical point $\xi_c \equiv \xi_N$ is reached. There, the transition $1 \to 0$ takes place and the system acquires an almost untwisted configuration.

In the insert of Fig. 3 an enlargement of the region of transitions for a system with $N=4$ twists is shown. It is clearly visible the first transition $4 \to 3$ [from branch $(m=0) \to (m=1)$ at $\xi_1^* = 0.0717$], while the successive transitions $3 \to 2 \to 1 \to 0$ corresponding to the branch jump $(m=1) \to (m=2)$, $(m=2) \to (m=3)$, and $(m=3) \to (m=4)$ occur, respectively, at $\xi_2^* = 0.0518$, $\xi_3^* = 0.0507$, and $\xi_c \equiv \xi_4^* = 0.0506$. They are too close to be distinguished in the picture.

Furthermore, we observe that for each branch of order $m > 0$ there are two possible energy curves corresponding to the down-layer, with $m\pi < \delta < (m+1/2)\pi$ and to the up-layer with $(m+1/2)\pi < \delta < (m+1)\pi$. The corresponding energy values are almost superimposed and not distinguishable in the figure, although the up-layer energy is lowest to the down-layer energy. Consequently, when a $(m-1) \to m$ transition occurs, the pitch angle at the boundary surface is always between $m\pi/2 < \delta < m\pi$.

In Fig. 4 we plot, for the case of $N=4$, the projection of the nematic director $\boldsymbol{n}(\zeta)$ along the $\boldsymbol{j}$ direction: $n_y(\zeta)\boldsymbol{n}(\zeta)\cdot\boldsymbol{j}$ for three different values of the distorting field ξ. In Fig. 4(a), the value of the field $\xi > \xi_1^*$ and the system has the whole twists number. It is also evident that in this situation the total twist angle $\Delta\varphi > N\pi$. In Fig. 4(b), the value of field $\xi_2^* > \xi > \xi_1^*$ and the system shows, as expected, only two complete twists. Finally, Fig. 4(c) depicts a case with $\xi < \xi_0^* \equiv \xi_c$. The configuration of the system is almost nematic and the residual distortion is concentrated at the right-hand side boundary, according to Eq. (2.10).

It is worthy to remark that, beside the energy curves depicted in Fig. 3 there are an infinite series of highest-energy curves corresponding to the branches of negative order. They are not illustrated in the figure for sake of clarity. We have verified that all energy curves corresponding to branches of negative order have energy values higher that those corresponding to $0 \leqslant m \leqslant N$ branches. They represent possible configurations of the system with a number of twists larger than N that are energetically unstable. We can discuss in a more heuristic manner the CLC $\to$ NLC transition looking at Eq. (4.3) as a function of the total twist angle $\Delta\varphi$ for fixed values of the distorting filed ξ. In Fig. 5, we plot several snapshots of the reduced total energy $\mathcal{G}[\varphi]$ vs $\Delta\varphi$ for a system with $N=4$ twists.

As can be seen, for large ξ the total energy assumes a parabolic shape with its minimum at $\Delta\varphi = 4\pi$ indicated by the arrow in Fig. 5(a). As the external field increases the parabolic shape ripples [Fig. 5(b)] and a minimum over the natural twist number appears. This is in agreement with the negative solution corresponding to the 0 branch. The situation changes suddenly as the distorting field grows. In fact, a first

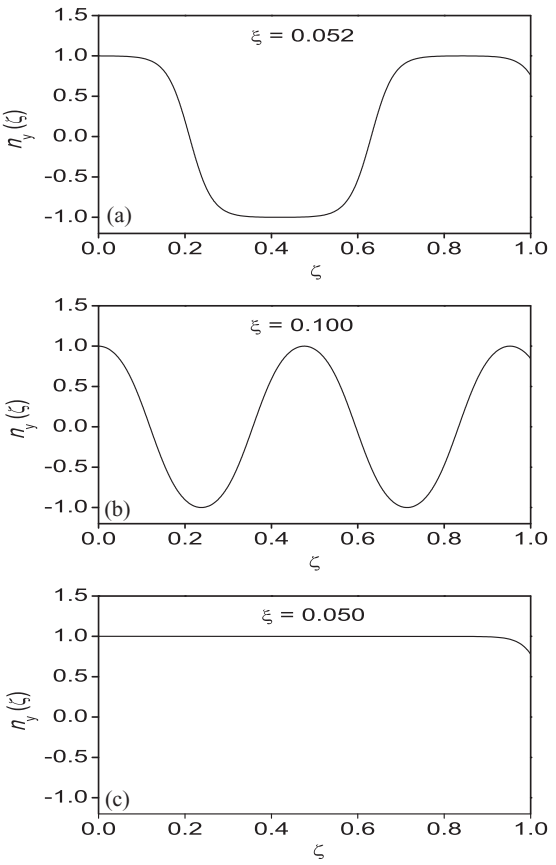

FIG. 4. y component of the nematic direction $n_y(\zeta) = \boldsymbol{n}(\zeta)\cdot\boldsymbol{j}$ vs ζ for three values of the distorting field.

minimum appears for $3\pi < \Delta\varphi < 4\pi$ [Fig. 5(c)], indicating a twist expulsion by the system [Fig. 5(d)]. When the external field approaches the critical value ξ_c, the reduced total energy shows a cascade of minima with almost the same absolute value [Fig. 5(e)]. A small increase of the external field produces an abrupt change in the position of the absolute minimum, indicating that twists are expelled in avalanche when the external field approaches the critical value ξ_c where the final cholesteric-nematic transition occurs. Finally, for larger and larger values of the field $\mathcal{G}[\varphi]$ is an almost increasing function of $\Delta\varphi$ with a unique minimum located at $\Delta\varphi \to 0$, where the system assumes an almost untwisted configuration [Fig. 5(f)].

We note that the situation illustrated above is very similar to the well-known phase transition phenomenon occurring in the Ising spin system controlled by the external temperature, where the reduced total energy $\mathcal{G}[\varphi]$ plays the role of the free energy for the given problem, the total twist angle the role of the controlling order parameter like the magnetization does in the Ising system and, of course, the external field ξ is identified with temperature.

Finally, in Fig. 6, we depict the same situation illustrated in Fig. 5 for a more realistic system with $N=20$ twists. In this case, it is evident that after the firsts few transitions the shape of the reduced total energy assumes a configuration with a series of minima having almost all the same value. In this situation a small variation in the strength of the external field produces a sudden variation in the position of the absolute minimum,

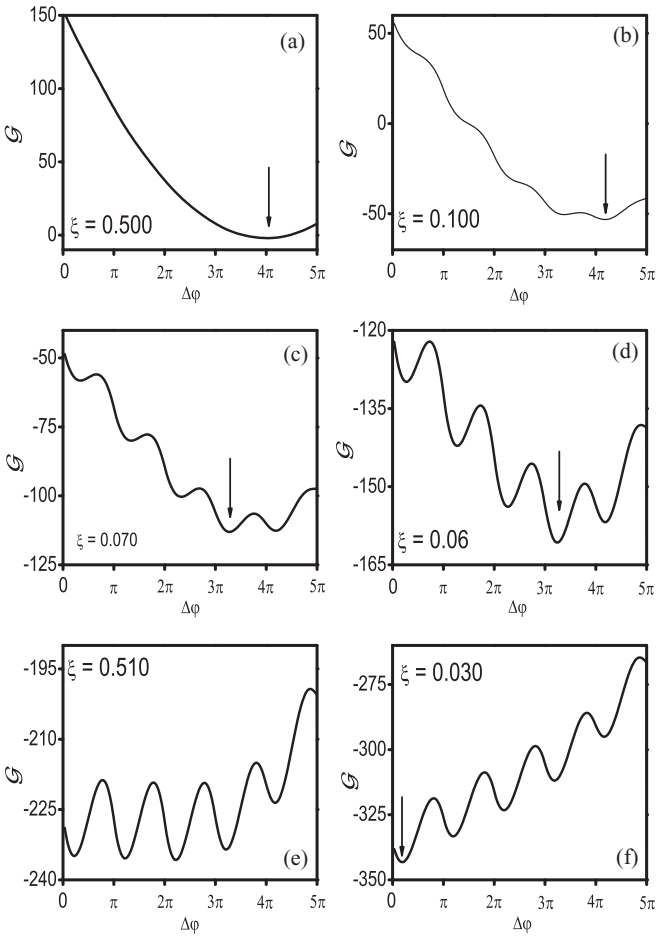

FIG. 5. Reduced total energy for a system with $N = 4$ twists vs the total twist angle for several values of the external field. The arrow indicates the position of the minimum minimorum when unique.

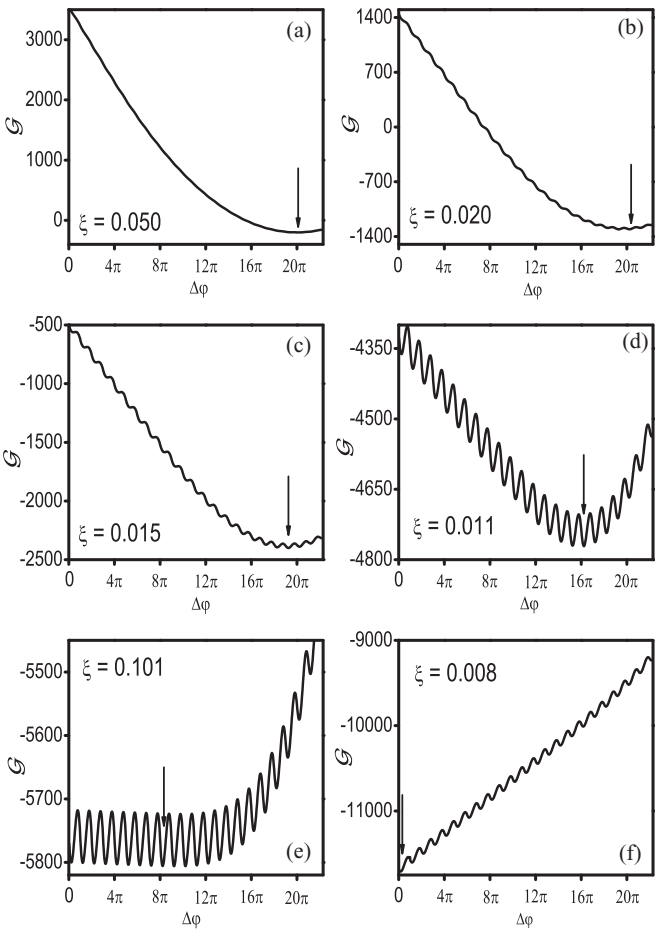

FIG. 6. Reduced total energy for a system with $N = 20$ twists vs the total twist angle for several value of the external field. The arrow indicates the position of the minimum minimorum when unique.

indicating the onset of twist expulsions in avalanche that deals the system toward the final nematic configuration.

VI. WEAK-WEAK ANCHORING CELL

Let us briefly discuss the generalization of our model to the case of a symmetric free cell system of finite thickness whose anchoring energy is negligible on both limiting surfaces.

The system is now described by Eq. (2.7), which still admits the first integral (3.1), together with the boundary conditions

$$\left.\frac{d\varphi}{d\zeta}\right|_0 = \left.\frac{d\varphi}{d\zeta}\right|_1 = \frac{\pi}{\lambda}. \tag{6.1}$$

Following the same steps described in Sec. III, we arrive consistently at the following condition for the pitch angle at the two limiting surfaces:

$$\kappa = \left(\frac{\pi}{\lambda}\,\xi\right)^2 - \sin^2\varphi(0) = \left(\frac{\pi}{\lambda}\,\xi\right)^2 - \sin^2\varphi(1), \tag{6.2}$$

which implies the relation

$$\sin\varphi(0) = \pm\sin\varphi(1). \tag{6.3}$$

By putting $\delta \equiv \varphi(0)$, with $\delta \to 0$ for $\xi \to \infty$, and accounting for the geometry of the problem we get

$$\varphi(1) = N\,\pi \pm \delta. \tag{6.4}$$

The first solution, $\varphi(1) = N\,\pi + \delta$, corresponds to a simple rotation of the system around the helical axis, because the total twist angle $\Delta\varphi = N\,\pi$ does not depend on δ. This case is not relevant for our goal and will be ignored.

Conversely, the second solution, $\varphi(1) = N\,\pi - \delta$, describes the distortion of the system since

$$\Delta\varphi = N\,\pi - 2\,\delta, \tag{6.5}$$

and we have a variation on the number of twist whenever δ increases or reduces of $\pi/2$.

Solutions for δ follows from the integral equation:

$$\int_\delta^{N\,\pi-\delta} \frac{d\varphi}{\sqrt{\left(\frac{\pi}{\lambda}\,\xi\right)^2 - \sin^2\delta + \sin^2\varphi}} = \frac{1}{\xi} \tag{6.6}$$

and can be written as

$$f(\xi, N\,\pi - \delta) - f(\xi, \delta) = \frac{1}{\xi}. \tag{6.7}$$

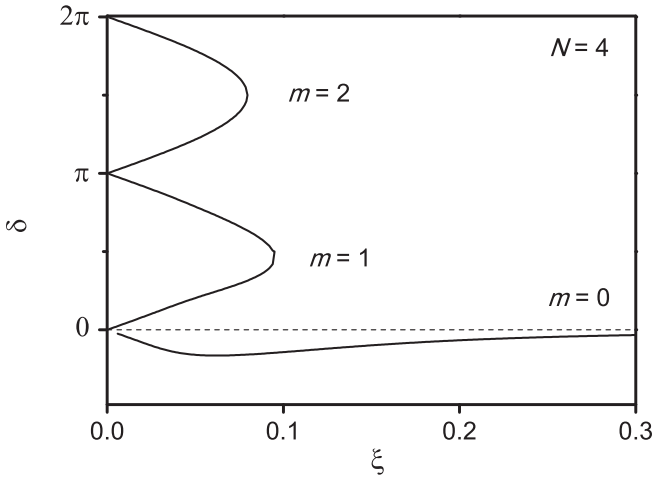

FIG. 7. Shape of δ vs ξ for a weak-weak anchoring cell system with $N = 4$ twists. Solutions corresponding to $m < 0$ are not plotted. The dashed line represents the asymptotic behavior of the main solution ($m = 0$) for $\xi \to \infty$.

We report, in Fig. 7, the solutions of this equation for a system with $N = 4$ twists vs the distorting field ξ. Like the case discussed in the previous section, negative branch solutions are unlimited and represent the case of increasing total twist number. These solutions are energetically unstable and are not reported in the figure. On the contrary, positive branch solutions are half in number with respect to the strong-free anchoring cases, i.e., $0 \leqslant m \leqslant [N/2]$, where $[x]$ is the nearest integer to x. They represent a situation in which the system reduces the total twist number, but now the expulsion occurs from both sides so the total twist number reduces by unity when δ varies by only $\pi/2$ instead of π. It is then clear from Fig. 7 that when a branch of highest order becomes available the jump of δ is greater than $\pi/2$ so the system expels more than one twist at a time. This is the main difference with the strong-weak anchoring case.

We can better observe this difference looking at the reduced total energy per unit surface, which in a weak-weak anchoring system is given by

$$\mathcal{G}[\varphi] = \int_{\delta}^{N\pi-\delta} \left[\left(\frac{d\varphi}{d\zeta} - \frac{\pi}{\lambda} \right)^2 - \frac{1}{\xi^2} \cos^2 \varphi \right] \frac{d\varphi}{\varphi'}, \qquad (6.8)$$

where now $\delta = \delta(\xi)$ is a solution of the boundary condition (6.7) and can be rewritten as

$$\mathcal{G}[\varphi] = -\frac{1}{\xi^2}(1+\kappa) + \frac{\pi}{\lambda}\left[\frac{\pi}{\lambda} - 2(N\pi - 2\delta)\right] + 2\frac{\sqrt{\kappa}}{\xi}\left(\mathcal{E}\left(N\pi - \delta, -\frac{1}{\kappa}\right) - \mathcal{E}\left(\delta, -\frac{1}{\kappa}\right)\right). \qquad (6.9)$$

Again, the stable configuration for a given value of the external field corresponds to the minimum minimorum of the energy levels (6.9), evaluated among the available branches.

Without entering into a detailed discussion that otherwise follows formally the same argumentation developed in the free-strong anchoring case, we can illustrate easily the cholesteric-nematic transition in the weak-weak anchoring case by looking at the reduced total energy vs the total twist angle.

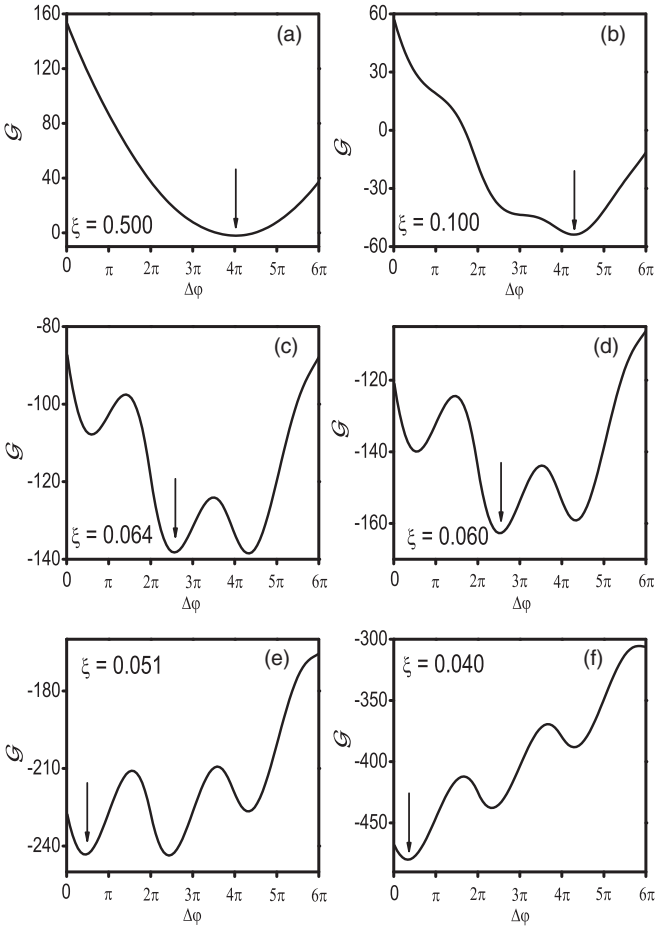

FIG. 8. Reduced total energy for a weak-weak anchoring cell system with $N = 4$ twists vs the total twist angle for a few values of the external field. The arrow indicates the position of the minimum minimorum.

This is illustrated in Fig. 8 where we plot several snapshots of $\mathcal{G}[\varphi]$ vs $\Delta\varphi$ for a weak-weak anchoring system with $N = 4$ twists. Starting from Fig. 8(a), we see that for large ξ the total energy has a parabolic shape with its minimum at $\Delta\varphi = 4\pi$. As the external field increases the parabolic shape ripples and move toward highest $\Delta\varphi$, indicating an increasing in the total twist angle [Fig. 8(b)]; this is in correspondence with the negative solution of the 0 branch. Increasing further the strength of the distorting field, a first minimum appears at $\xi_1^* = 0.064$ [Fig. 8(c)] with a pitch angle variation $\Delta\delta \approx 2\pi$, indicating a twist expulsion of $4 \to 2$ [from branch $(m = 0) \to (m = 1)$; Fig. 8(d)]. The situation repeats at the next expulsion point that occurs at $\xi_2^* \equiv \xi_c = 0.051$ [Fig. 8(e)], where the system expels two twists again, passing to $2 \to 0$ and corresponding to $(m = 1) \to (m = 2)$. After that, for larger and larger fields, $\mathcal{G}[\varphi]$ is an almost increasing function with a unique minimum located at $\Delta\varphi \to 0$ where the system assumes an almost untwisted configuration [Fig. 8(f)].

VII. CONCLUSIONS

We have studied a CLC cell of finite thickness in strong-weak anchoring under the influence of an external field. It has been shown that as the strength of the distorting field

increases the twist angle at the limiting surface varies in a series of discrete steps whereby the system expels a twist once in a sequence that suddenly reaches a critical value ξ_c and beyond which it assumes a nematic configuration. We have also generalized our study to the case of a system in a cell of finite thickness in weak-weak anchoring, showing that this transition occurs almost in the same way, with the relevant difference that now twists are expelled twice at a time.

This work is a natural continuation of the previous studies [28,29], where a cell of CLC with finite thickness with a strong anchoring at the limiting surfaces is perturbed by an external field. In that case it also has been shown how the system expels twists one by one in a sequence that accumulates toward the critical value, signifying the CLC → NLC final transition.

As we have widely discussed in Sec. III, the boundary conditions give rise to a complex set of possible solutions at the limiting surfaces that make the study of the free cell system more complicated than the corresponding strong anchoring problem. In this paper we have considered just the equilibrium configuration corresponding to the state with the minimal energy between the possible configurations. However, in presence of thermal fluctuations the situation may change drastically. In fact, as shown in the previous section, when the external field increases, a series of local minima appears in the reduced total energy. These minima are separated by an energy gap. In a dynamical analysis the transition from a configuration with n twists to near a configuration with $n-1$ twists necessitates that the energy gap is overcome. The probability transition from the two configurations depends on the gap width and on the temperature of the system and decreases as the temperature decreases. Therefore, in a low-temperature system, the CLC → NLC transition could be statistically improbable and the system cold stay "frozen" in the cholesteric configuration also for distorting field strength beyond the critical value. We will analyze the temperature effect on the cholesteric-nematic transition in later work.

In our analysis the anisotropic part of the surface energy is assumed to be very large or very small with respect to the total energy per unit surface due to the bulk distortion induced by the magnetic field. In this framework the functional form of the surface energy is inessential. The particular case where the anisotropic part of the surface energy is comparable with that related to the distortion induced by the magnetic field can be analyzed by assuming a well-defined form for the functional form for the surface energy. The analysis of the CLC → N transition in this case can be investigated by means of the general formulas reported in our paper.

[1] L. M. Blinov, *Structure and Properties of Liquid Crystals* (Springer, Berlin, 2001).

[2] Z. Hotra *et al.*, Mol. Cryst. Liq. Cryst. **535**, 225 (2011); **534**, 32 (2011).

[3] I. Gvozdovskyy, O. Yaroshchuk, and M. Serbina, Mol. Cryst. Liq. Cryst. **546**, 202 (2011).

[4] I. I. Smalyukh, B. I. Senyuk, P. Palffy-Muhoray, O. D. Lavrentovich, H. Huang, E. C. Gartland, Jr., V. H. Bodnar, T. Kosa, and B. Taheri, Phys. Rev. E **72**, 061707 (2005).

[5] A. G. Kozachenko and L. Komitov, Mol. Cryst. Liq. Cryst. **412**, 205 (2004).

[6] Y. Yabe and D. S. Seo, Mol. Cryst. Liq. Cryst. **357**, 1 (2001).

[7] L. J. M. Schlangen, A. Pashai, and H. J. Cornelissen, J. Appl. Phys. **87**, 3723 (2000).

[8] R. R. Swisher, H. Huo, and P. P. Crooker, Liq. Cryst. **26**, 57 (1999).

[9] S. V. Shiyanovskii and J. G. Terentieva, Liq. Cryst. **21**, 645 (1996).

[10] Y. Yabe and D. S. Seo, Liq. Cryst. **17**, 847 (1994).

[11] P. J. Kedney and I. W. Stewart, Lett. Math. Phys. **31**, 261 (1994).

[12] A. Mochizuki and S. Kobayashi, Mol. Cryst. Liq. Cryst. **225**, 89 (1993).

[13] Z. A. de SantAna, and A. M. Figueiredo Neto, Phys. Rev. A **46**, 7630 (1992).

[14] V. L. Golo and E. I. Kats, Zh. Éksp. Teor. Fiz. **55**, 275 (1992) [JETP Lett. **55**, 273 (1992)].

[15] Z. Y. Gotra *et al.*, Liq. Cryst. **9**, 893 (1991).

[16] J. Prost and P. G. de Gennes, *The Physics of Liquid Crystals*, (Clarendon Press, Oxford, 1994).

[17] P. G. de Gennes, Solid State Commun. **6**, 163 (1968).

[18] R. B. Meyer, Appl. Phys. Lett. **12**, 281 (1968).

[19] G. Durand, L. Leger, I. Rondelez, and M. Veyssie, Phys. Rev. Lett. **22**, 227 (1969).

[20] R. B. Meyer, Appl. Phys. Lett. **14**, 208 (1969).

[21] R. Dreher, Solid State Commun. **13**, 1571 (1973).

[22] P. J. Kedney and I. W. Stewart, Continuum Mech. Thermodyn. **6**, 141 (1994).

[23] V. A. Belyakov, JETP Lett. **76**, 88 (2002).

[24] S. V. Belyaev and L. M. Blinov, JETP Lett. **30**, 99 (1979).

[25] E. Niggemann and H. Stegemeyer, Liq. Cryst. **5**, 739 (1989).

[26] P. Oswald, J. Baudry, and S. Pirkl, Phy. Rep. **337**, 67 (2000).

[27] I. Lelidis and P. Galatola, Phys. Rev. E **66**, 010701 (2002).

[28] A. M. Scarfone, I. Lelidis, and G. Barbero, Phys. Rev. E **84**, 021708 (2011).

[29] I. Lelidis, G. Barbero, and A. M. Scarfone, Centr. Eur. J. Phys. **10**, 587 (2012).

[30] G. Barbero and L. R. Evangelista, *An Elementary Course on the Continuum Theory for Nematic Liquid Crystals* (World Scientific, Singapore, 2000).

[31] A. Rapini and M. Papoular, J. Phys. Colloque **30**, C4-54 (1969).

[32] M. Kleman, *Points, Lignes, Parois* (Les Editions de Physics, Les Ulis, France, 1977).

[33] M. Abramowitz and I. A. Stegun, *Handbook of Mathematical Function* (Dover, New York, 1970).